J. Fluid Mech. (1986), *vol.* 168, *pp.* 119–150
Printed in Great Britain

Rheo-optical studies of the effect of weak Brownian rotations in sheared suspensions

By PAUL L. FRATTINI AND GERALD G. FULLER
Department of Chemical Engineering, Stanford University, Stanford, CA 94305, USA

(Received 15 July 1985)

The orientation state of a dilute suspension of rigid, axisymmetric particles subjected to the sudden inception of simple shearing flow in the presence of small Brownian couples is investigated experimentally. In contrast to mechanical rheometric methods, the experimental technique, a recently developed optical method based on conservative linear dichroism (Frattini & Fuller 1984), provides a direct probe of the constituent particle dynamics. The average particle orientation direction projected into the shear plane and the average degree of alignment about that direction are measured as functions of time for Péclet numbers, $\dot{\gamma}/D_r$, ranging from 20 to 200. Data are presented for dilute glycerol/water suspensions of two types of particles: disk-like bentonite clay and rod-like synthetic akaganeite (βFeOOH). The data provide, for the first time, an experimental basis with which the closure approximation required for solution of the evolution equation for $\langle \boldsymbol{u}, \boldsymbol{u} \rangle$, the second moment of the particle orientation distribution, may be critically evaluated in shearing flows. Two closures are examined: the *ad hoc* but often-used pre-averaging closure, and the first-order closure suggested by Hinch & Leal (1976). The latter results in a more accurate fit of the data. Finally, new experimental observations of the effect of particle size polydispersity are reported for the orientation relaxation following sudden cessation of steady simple shear at moderately high Péclet number.

1. Introduction

The creeping motion of a single, freely suspended particle in a Newtonian fluid subjected to simple shear has been the topic of much theoretical and experimental work in the more than sixty years since Jeffery published his classic paper (1922). In that work, Jeffery solved the Stokes equations for the motion of a freely suspended spheroid in simple shear and found that, in addition to translating with the local flow field, the particle undergoes indefinite rotation through a closed orbit about the free-stream vorticity. The major axis of the particle traces through one member of a single-parameter family of closed curves; the particular orbit in which a particle finds itself at any time after the inception of flow depends upon its initial orientation. The period of revolution through a Jeffery orbit is a function of the particle aspect ratio r, with the period increasing proportionately as $(r+1/r)$. The orbit velocity is a nonlinear function of particle orientation. The major axis of a prolate particle ($r > 1$), for example, rotates more slowly through orientations near the direction of flow than through the direction normal to it. The converse holds for oblate spheroids ($r < 1$).

Consider a dilute suspension of non-interacting Jeffery spheroids initially at rest; that is, the particles have overall obtained a random orientation state. If a simple

shear flow is then imposed on this suspension, a time-varying orientational anisotropy is induced in the suspension as a consequence of the nature of the Jeffery rotations. The orientation state oscillates indefinitely between a random distribution and a distribution corresponding to the maximum degree of alignment induced by the flow. The maximum induced anisotropy depends upon the particle aspect ratio and varies from a state of negligible orientation for nearly spherical particles to complete alignment as $(r+1/r)\rightarrow\infty$.

The optical properties of such a sheared suspension, in particular the refractive-index tensor, are functions of the particle orientation state induced by the flow. A real-time measurement of flow-induced anisotropy in any optical property, then, provides an experimental observable through which the orientationally averaged particle dynamics may be inferred. Let the probability density for finding a particle with its major axis oriented along a direction between $\boldsymbol{u}$ and $\boldsymbol{u}+\mathrm{d}\boldsymbol{u}$ at a time between t and $t+\mathrm{d}t$ be denoted by $\Psi(\boldsymbol{u},t)$. In general, the optical anisotropy induced in the suspension is related to the moments of $\Psi(\boldsymbol{u},t)$ via an appropriate light-scattering theory. The equation of motion describing the time evolution of $\Psi(\boldsymbol{u},t)$ depends explicitly on the forces which determine the particle dynamics. For example, Ψ has been derived in closed form (Okagawa, Cox & Mason 1973) directly from Jeffery's solution for a dilute suspension of spheroids subjected to simple shear from rest. In sum, optical data provide measurements of certain moments of Ψ which in turn can often be used to critically evaluate theoretical treatments of particle dynamics in suspension rheology.

Since most rheo-optical methods of interest can be characterized as transmission experiments, we consider the suspension dynamics of the Jeffery problem projected into the shear plane. The optically neutral axis (which lies along the direction of light propagation) then coincides with the vorticity of the imposed flow. In this configuration, the net anisotropy induced in the suspension can be completely characterized by two observables: the average orientation direction of the major axis of the particles projected into the shear plane (given by the angle χ measured with respect to the flow direction), and the degree of alignment of the particles about that direction, Δf. Both χ and Δf are functions of time and in general both quantities are required in order to describe unambiguously the orientation state of the suspension. The degree of alignment varies from zero for the random state to unity in the case of complete particle alignment, and χ is normally reported in one quadrant $[-\frac{1}{4}\pi,\frac{1}{4}\pi]$.

Measurement of the magnitude and the extinction direction of flow-induced optical anisotropy can provide a direct determination of Δf and χ respectively. The classic example of this type of experiment is the measurement of flow-induced birefringence; or equivalently, anisotropy in the real part of the refractive-index tensor of the suspension. The birefringence method has been applied extensively to the study of the rheology of polymeric liquids (see, for example, the review by Leal 1984) and to some extent to colloidal sols consisting of crystallites of size less than a micrometre (reference the review by Peterlin 1976). For a number of reasons, however, the method is inappropriate for the micrometre-size particles to which the Jeffery analysis would normally apply in a typical experimental situation. The principal reason is the dominance of scattering over retardation in the visible-wavelength range for the larger particles.

Even though the Jeffery problem has been studied extensively by Mason and co-workers using direct photographic methods (Anczurowski & Mason 1967*a*, *b*, and subsequent work), little experimental work has been undertaken to investigate important effects which perturb the Jeffery motion, largely for lack of a feasible

experimental technique. Such effects include Brownian motion, hydrodynamic interactions (Kim 1985 and references therein) or colloidal particle interactions, effects of non-Newtonian suspending fluids (Brunn 1980; Leal 1979), and effects of externally imposed fields (for example, electric fields: Van de Ven 1984). These problems are not only of fundamental interest but also of practical importance in that the orientation state induced during processing affects the ultimate bulk properties of such products as fibre-reinforced materials and magnetic information-storage media.

Recently, an optical method which takes advantage of the polarization anisotropy in total, forward scattering (turbidity) from a flowing suspension of non-spherical particles has been developed which makes possible experimental investigations of many of those problems associated with perturbations in the Jeffery particle motion (Frattini & Fuller 1984). Straightforward turbidity measurements have been used for some time to study the Jeffery problem, particularly the phase-mixing effect which results from polydispersity in particle aspect ratio (for example, Cerda, Foister & Mason 1981). The turbidity experiment, however, is insensitive to changes in the orientation angle χ and therefore is not suitable for studying many of the suggested problems. Instead of measuring turbidity differences directly, the method of Frattini & Fuller measures a related property; namely, the magnitude and the extinction direction of flow-induced conservative linear dichroism (equivalently, anisotropy in the imaginary part of the refractive-index tensor of the suspension). The details of this technique are outlined in §2 of this paper. In a manner analogous to the birefringence experiment for polymeric liquids, these data provide direct, time-dependent measures of both Δf and χ for suspensions.

In this paper, we report the results of experimental investigations into the effect of small Brownian couples on the dynamics of dilute suspensions of Jeffery particles in simple shear flow using the linear-dichroism technique. We suppose that even though Brownian diffusion is small, it still dominates other effects which perturb particle orbital motion, such as inertia, non-Newtonian solvent effects, and particle–particle interactions. These other effects, however, may also be specifically selected for detailed study, using the same optical method, by an appropriate choice of experimental conditions. The reports given here of data on the weak-Brownian-motion problem in simple shear, then, serve to demonstrate the utility of the dichroism technique in suspension rheology. In fact, an objective of this work, which is as important as the experimental investigations, is to illustrate the method by which these optical data can be interpreted in terms of theories of particle dynamics.

The weak-Brownian-motion problem represents an opportunity for experimental studies of particle dynamics both in the context of evaluating current theoretical treatments of the problem and from the point of view of using flow data in conjunction with the salient features of these theories to investigate the physical properties of uncharacterized suspensions. Several important features of the weak Brownian motion in simple shear flow make this choice of flow field particularly interesting. First of all, only a small amount of Brownian diffusion is required to significantly alter even the qualitative nature of the particle motion (Leal & Hinch 1971). Since the bulk stress in the suspension is a strong function of the particle orientation, the bulk rheological properties of the suspension can be significantly affected by changes in the orientation state induced by weak diffusion. To date, there has not been any experimental study which focuses on the microdynamics of this problem. Secondly, the applicability of the conclusions drawn extends beyond just systems of spheroids in simple shear. With a few esoteric exceptions, the zero-Reynolds-number rotational

dynamics of any body of revolution is mathematically identical to that of a spheroid provided an equivalent aspect ratio is correctly defined (Bretherton 1962). We take advantage of this fact experimentally as well in that truly spheroidal particle systems are almost impossible to obtain in practice. In addition, the simple shear results may be extended to any two-dimensional flow with strain rate E and vorticity 2Ω in which the particle orbits are closed provided Pe, the Péclet number (normally $\dot{\gamma}/D_r$, where $\dot{\gamma}$ is the shear rate and D_r the rotary diffusivity), is replaced by $2\Omega/D_r$ and the aspect ratio is redefined as r^* (Hinch & Leal 1972):

$$(r^*)^2 = \frac{(r^2+1)\,\Omega + (r^2-1)\,E}{(r^2+1)\,\Omega - (r^2-1)\,E}.$$

Thirdly, a closed-form solution for $\Psi(\boldsymbol{u}, t)$ has been elusive when the imposed flow contains vorticity despite significant theoretical effort on the small-Brownian-diffusion problem. The analysis to date has focused on the development of perturbation solutions and is also often restricted to extreme-aspect-ratio particles. In general, the computation involved in evaluating these slowly converging series for comparison with experimental data becomes unwieldy since not only Ψ but also its moments must be evaluated and then integrated to account for experimentally observed polydispersity in particle size and aspect ratio. For the purposes of this paper, the major contribution of this theoretical work is the elucidation of the underlying physical features of the problem (Hinch & Leal 1973, 1972; Leal & Hinch 1972, 1971). Knowledge of these features aids in qualitative interpretation of the optical data, and we therefore summarize them here.

At long times, Leal & Hinch (1971) found that small Brownian couples eventually force a complete redistribution of particle orbits toward a steady-state orbit distribution which is independent of the initial suspension configuration, thus removing the so-called indeterminacy in the Jeffery problem. Scheraga, Edsall & Gadd (1951) first calculated the steady-state orientation angle and birefringence function for $\dot{\gamma}/D_r < 60$ by evaluating many terms of the classic strong-Brownian-motion series of Peterlin. Brenner (1974) has summarized and extended many of the available steady-state results. Hinch & Leal (1972) also pointed out a specific aspect-ratio dependence to the strength of the Brownian perturbations, for a given $\dot{\gamma}/D_r$, which is a consequence of the orientation dependence of the Jeffery rotation velocity. $D_r/\dot{\gamma} \ll 1$ is a necessary but not a sufficient condition for hydrodynamic forces to dominate Brownian diffusion at all orientations. For highly anisometric particles, the orientational probability distribution of the major axis of the particles is sharply peaked near the flow direction when $r \gg 1$, or normal to it when $1/r \gg 1$. Since the strength of the Brownian perturbations is proportional to gradients in orientation space, the large local gradients which result may lead to a singular region near the alignment direction in which hydrodynamic effects and rotary diffusion are comparable even when $\dot{\gamma}/D_r \gg 1$. The additional condition which assures that Brownian motion is uniformly weak is $\dot{\gamma}/D_r \gg (r+1/r)^3$ (Hinch & Leal 1972). Thus, the explicit aspect-ratio dependence of the *local* Péclet number is quite strong. Data are presented in this paper for two particle systems with different average aspect ratios in order to investigate both the uniformly weak regime and the intermediate regime.

The experimental results reported in this paper consider the complete time-dependent problem in simple shear from the inception of flow to the approach toward steady state. The multiple timescales inherent in the full problem for $\Psi(\boldsymbol{u}, t)$ have

limited the analysis in simple shear largely to the construction of approximate solutions for nearly spherical particles (Leal & Hinch 1972) and extreme-aspect-ratio particles (Hinch & Leal 1973). The near-sphere problem is of little experimental interest in this work because the optical anisotropy of the suspension decays to zero rapidly as the particles approach spherical shape. Since the linear-dichroism method is otherwise applicable to time-dependent studies of induced particle orientation, we summarize here the important qualitative features as $r \to \infty$. Hinch & Leal (1973) delineate three temporal stages to the diffusive damping of the oscillations characteristic of Jeffery motion. For times $\dot{\gamma}t \leqslant Pe/r^4$, the Jeffery orbit motion proceeds essentially unperturbed. In the region $Pe/r^4 \leqslant \dot{\gamma}t \leqslant Pe/r^2$, the distribution of particle orbits is not altered appreciably but the motion of the particles within their orbits is perturbed, resulting in a phase mixing about each orbit. Finally, for dimensionless time greater than Pe/r^2, Brownian motion acts to redistribute the relative population of the orbits until a steady configuration is obtained. In addition, the polydispersity in particle shape present in practice introduces a phase mixing in the experimental observables since the period of a particle's orbit depends upon its aspect ratio. Generally, the characteristic time for this damping will exceed $(D_r r^2)^{-1}$, and therefore, phase mixing due to shape polydispersity often confounds interpretation of the experimentally observed oscillations.

Finally, the data given in this experimental study of the weak-Brownian-motion problem present a unique opportunity to evaluate the closure approximation normally employed in solving directly for $\langle \boldsymbol{u}\,\boldsymbol{u} \rangle$, the second moment of $\Psi(\boldsymbol{u}, t)$. The well-known alternative to first solving for Ψ and then calculating $\langle \boldsymbol{u}\,\boldsymbol{u} \rangle$ is to generate a differential equation for the time evolution of the second moment by suitable integration of the Fokker–Planck equation describing Ψ and then to solve this evolution equation directly for $\langle \boldsymbol{u}\,\boldsymbol{u} \rangle$. This procedure, however, generates a classic closure problem; namely, the equation for $\langle \boldsymbol{u}\,\boldsymbol{u} \rangle$ depends explicitly on $\langle \boldsymbol{u}\,\boldsymbol{u}\,\boldsymbol{u}\,\boldsymbol{u} \rangle$, and so on to higher orders. This problem appears in many other areas of rheology, as well as in many other fields. Typically, to expedite the calculation procedure, particularly in process simulations, the simplest decoupling approximation is implemented

$$\langle \boldsymbol{u}\,\boldsymbol{u}\,\boldsymbol{u}\,\boldsymbol{u} \rangle : \mathbf{E} \simeq \langle \boldsymbol{u}\,\boldsymbol{u} \rangle \langle \boldsymbol{u}\,\boldsymbol{u} \rangle : \mathbf{E}, \text{ the pre-averaging approximation (PA).}$$

For the weak-Brownian-motion problem with an imposed simple shear, however, the PA approximation is completely *ad hoc* and therefore can produce anomalies in the calculations. Despite this fact, it is often used in practice in similar problems with little justification. In this paper, we test this hypothesis experimentally from a microstructural point of view for the specific problem of a dilute suspension subjected to a simple shear flow in the presence of weak rotary diffusion. Hinch & Leal (1976, 1975) have studied various microstructurally based closures for this problem in a general linear flow field. They suggest a procedure for constructing a composite closure, valid at intermediate Péclet number, by interpolation between known strong-flow and weak-flow asymptotic forms for the second moment closure. In the case of simple shear, however, the limiting form for the closure at large Pe is unavailable. The first-order interpolation in this case (HL) amounts to matching a high-Pe approximation equivalent to the PA closure to the low-Pe asymptotic closure for simple shear flow. This HL closure might be expected to improve the accuracy of the PA approximate in simple shear since it obtains the correct slow flow limiting form. Of course, many of the strengths and weaknesses of each of these closures could be elucidated by intense numerical calculations of the type undertaken by Scheraga (1955) and more recently suggested again by Krushkal & Gallily (1984). Comparison

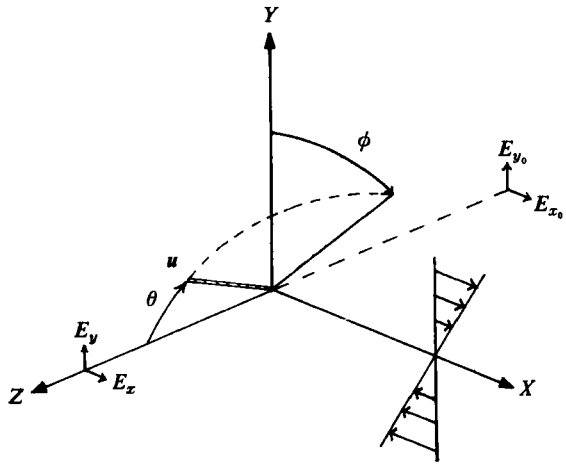

FIGURE 1. Coordinate system for a particle with major axis oriented at angles θ and ϕ. Light travels in the z-direction with incident electric vector $\boldsymbol{E}_0$. Light scattered in the forward direction has electric vector $\boldsymbol{E}$.

with experimental data on real particle systems, however, provides a much clearer indication of the accuracy and the utility of these methods.

The remainder of this work is organized and presented in five sections. In §2, we summarize the linear dichroism technique and discuss the physical properties of the suspensions employed in this study. In §3, model calculations of the experimental observables expected for a monodispersed suspension subjected to simple shear without Brownian motion are presented in order to evaluate both the HL and PA approximations in this limit where the orientation distribution function is known in closed form. The data are compared to calculations of $\langle \boldsymbol{u}\,\boldsymbol{u} \rangle$ using both closure approximations for simple shear flow in the uniformly weak (§4) and in the intermediate (§5) regimes of rotary diffusion. In the final section, data are presented which illustrate important qualitative effects of particle-size polydispersity during the suspension relaxation following cessation of steady simple shear at moderately high Péclet number.

2. Experimental method and materials

2.1. *The linear-dichroism technique*

Consider a suspension of rigid, spheroidal particles in a Newtonian fluid. The orientation of the major axis of each particle is given by the Euler angles θ and ϕ, and a simple shear flow $\dot{\gamma}(y, 0, 0)$ is imposed at some arbitrary time in the plane normal to the direction of propagation of the light, as shown in figure 1. The suspension is hydrodynamically dilute, and therefore also dilute enough to consider only single, independent scattering events. The intensity $|\boldsymbol{E}|^2$ of light scattered from the suspension will not only be a function of the particle-orientation state but also will depend on the state of polarization of the incident light. For an axially homogeneous optical medium, this polarization dependence is conveniently described in terms of a complex, second-rank tensor, $\langle \boldsymbol{n} \rangle$, the effective refractive index of the suspension. The angular brackets $\langle\rangle$ denote integration over the particle orientation distribution $\Psi(\theta, \phi, t)$ on the unit sphere. The magnitude of the linear polarization anisotropy in

the intensity of forward scattering is manifested as linear dichroism, $\Delta n''$. More precisely, $\Delta n''$ is the difference in the principal eigenvalues of $\mathrm{Im}(\langle \boldsymbol{n} \rangle)$, and the extinction direction χ is given directly by the orientation of the principal axis of $\mathrm{Im}(\langle \boldsymbol{n} \rangle)$. The degree of particle alignment, then, is simply $\Delta n''/\Delta n''_{\max}$, where $\Delta n''_{\max}$ denotes the magnitude of the dichroism in the fully aligned state.

In general, three sources of linear dichroism have been identified: dichroism due to polarization anisotropy in absorption, form dichroism due to the discontinuity in refractive index at a non-spherical particle–solvent interface, and conservative dichroism arising from the intrinsic optical anisotropy of the scattering medium. In this work, the latter effect dominates the form effect, and the particles, though uniaxally anisotropic in polarizability, are non-absorbing at the wavelength of light used in these experiments. Thus, the dichroism induced by shearing suspensions of such particles is predominantly conservative dichroism. To leading order in wave number, then, the orientational portion of $\mathrm{Im}(\langle \boldsymbol{n} \rangle)$ is calculated from the Rayleigh limit of the light-scattering problem:

$$\mathrm{Im}(\langle \boldsymbol{n} \rangle) = C_1 \langle \boldsymbol{u}\,\boldsymbol{u} \rangle + C_2 \boldsymbol{\delta},$$

where C_1 and C_2 are constants which depend on the optical properties of the particles and suspending medium. The degree of alignment and orientation angle are given in this approximation by

$$\left.\begin{aligned} \frac{\Delta n''}{\Delta n''_{\max}} &= [\langle \sin^2\theta \sin 2\phi \rangle^2 + \langle \sin^2\theta \cos 2\phi \rangle^2]^{\frac{1}{2}}, \\ \tan 2\chi &= \frac{\langle \sin^2\theta \sin 2\phi \rangle}{\langle \sin^2\theta \cos 2\phi \rangle}. \end{aligned}\right\} \tag{1}$$

Readers familiar with the classic birefringence experiment will recognize the birefringence function in (1). Birefringence and dichroism are directly proportional in the low-wavenumber limit. The magnitude of the dichroism for colloidal systems, however, often greatly exceeds the birefringence. Higher-order corrections to the scattering treatment produce only quantitative improvements in the calculations, especially in the case of χ (Frattini 1985), and their exclusion does not affect the validity of the conclusions drawn in this work even though the particle systems employed here do not strictly fall within the Rayleigh limit.

The quantities $\Delta n''$ and χ are measured simultaneously as functions of time. They provide a measure of the second moment of the orientation state induced in the suspension via (1). Unlike birefringence measurements on polymeric liquids for which the 'stress-optical law' applies, they do not provide a measure of the particle contribution to the stress since it is not strictly proportional to $\langle \boldsymbol{u}\,\boldsymbol{u} \rangle$. Any accurate microstructural model of the bulk rheological properties of a suspension, however, should necessarily be capable of predicting the average particle orientation direction and degree of alignment.

Figure 2 schematically illustrates the experimental apparatus used to measure $\Delta n''$ and χ as functions of time. The method has been described in full elsewhere (Frattini 1985; Frattini & Fuller 1984) and therefore only the major features are outlined here. The flow field is generated in a cylindrical Couette device with the He–Ne laser light beam propagating along the vorticity axis and with the flow direction assigned an orientation of $\chi = 0°$. The optical technique is based upon a polarization modulation scheme which has the unique capability of measuring $\Delta n''$ and χ simultaneously. The state of polarization of the light incident upon the flow cell is modulated at frequency

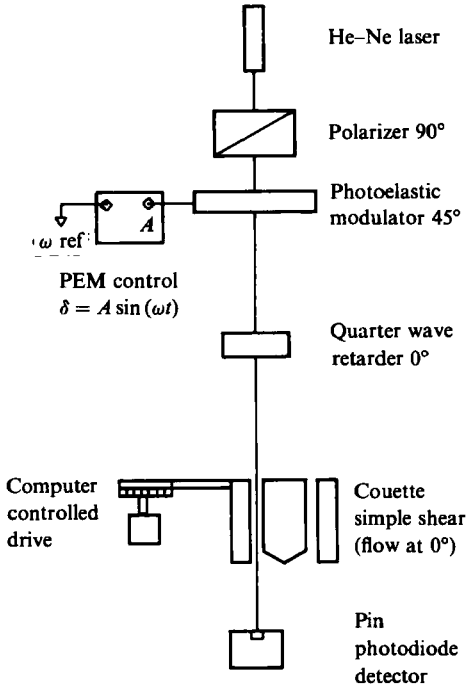

FIGURE 2. Schematic of the linear dichroism apparatus using a photoelastic modulator (PEM).

Property	Bentonite	Synthetic βFeOOH
Aspect ratio		
Average	0.45	6.29
% Dispersion	21 %	22 %
Lengthscale ($2a$)		
Average (μm)	2.07	1.23
% Dispersion	57 %	18 %
Concentration (p.p.m.–wt)	500	50
Hydrodynamic volume fraction	< 0.0005	< 0.0008
Suspending fluid		
Glycerol/water (v/v)	7/3 to 9/1	99/1
Viscosity (cp)	20 to 170	800
Temperature (C)	30 ∓ 0.3	25 ∓ 0.3
Relative particle refractive index (m)	≈ 1.02	≈ 1.63
Rayleigh-Gans wave-number: $ka(m-1)$	≈ 0.2	≈ 3.1
Intrinsic birefringence	$O(10^{-2})$†	$O(10^{-1})$‡

† Crystalline montmorillonite clay. ‡ α-phase of FeOOH.

TABLE 1. Suspension properties

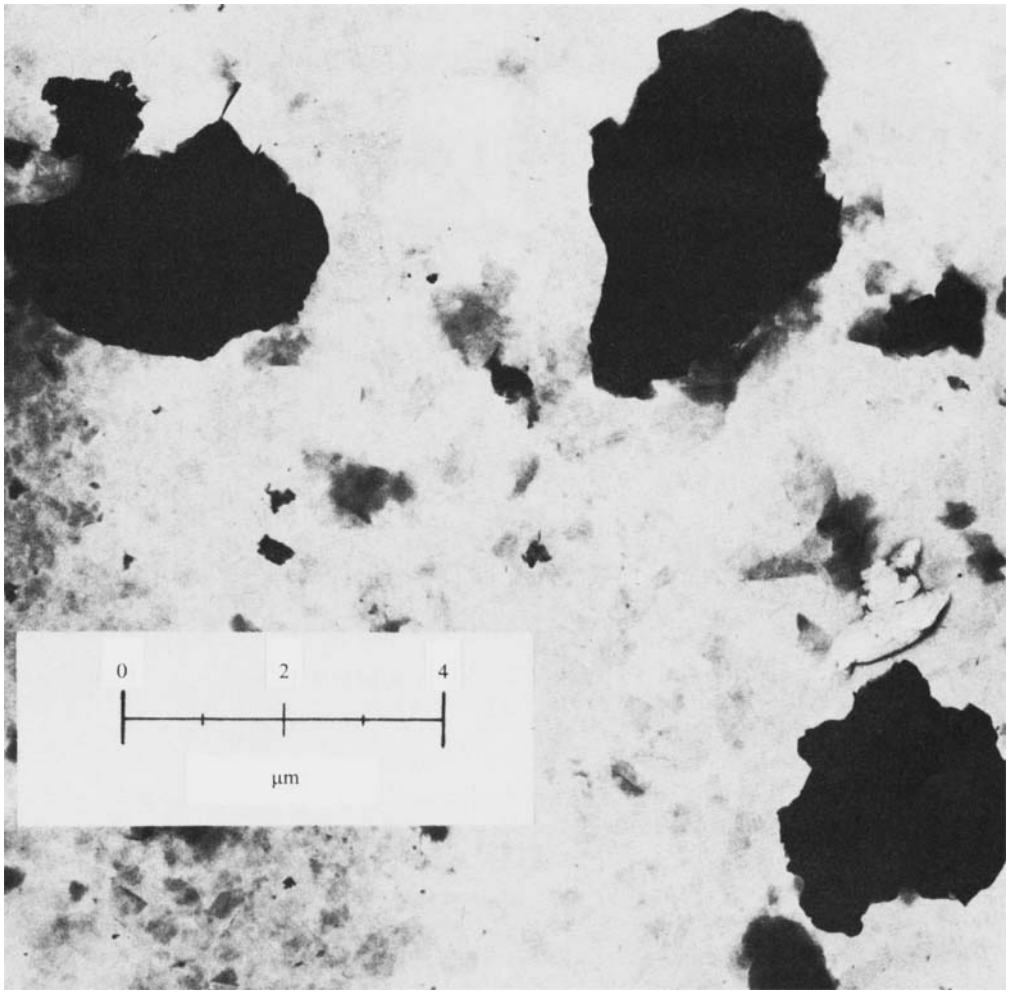

FIGURE 3. Transmission electron micrograph of sample particles from the Wyoming bentonite system.

ω (50.3 kHz) by a sequence of optical elements consisting of a linear polarizer at 90°, a photoelastic modulator (PEM) at 45° and a quarter wave retarder oriented at 0°. The PEM introduces a sinusoidally varying retardance $\delta_m = A \sin(\omega t)$ with fixed frequency but experimentally adjustable amplitude. At an appropriate amplitude, the first and second harmonics of the detected intensity, each normalized by the zero frequency intensity, are simple, independent functions of $\Delta n''$ and χ. The intensity signal is therefore demodulated in real time using an analog lock-in amplification scheme keyed on reference signals at ω and 2ω which are phase locked to the PEM. Both normalized harmonics are recorded and then inverted numerically to give $\Delta n''$ and χ as functions of time.

2.2. *Materials*

Glycerol/water suspensions of two different aspect-ratio particle systems were employed in this work. The details of the sample preparations may be found in

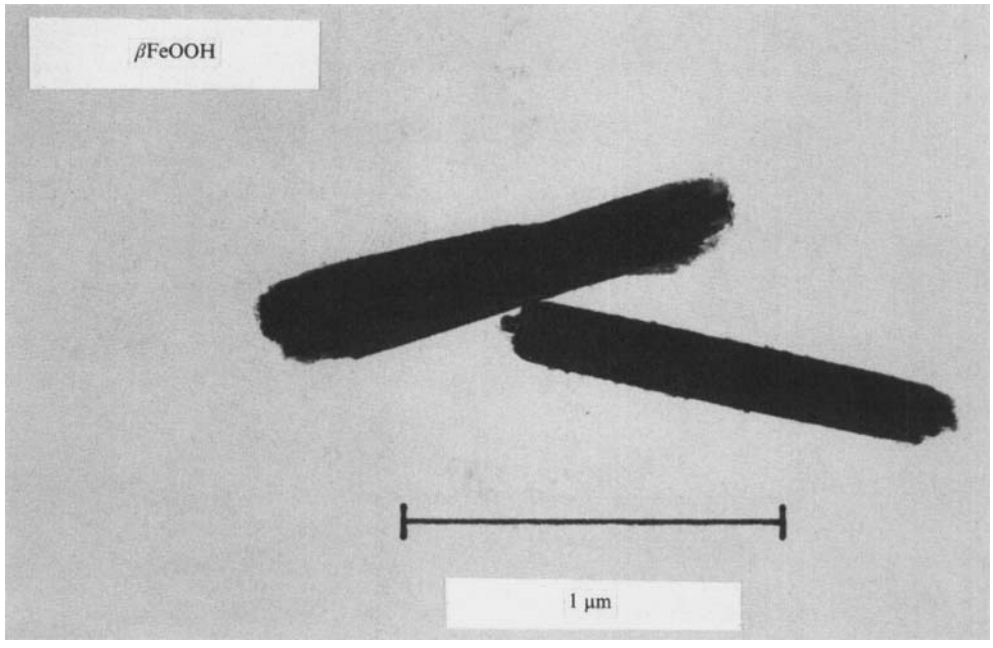

FIGURE 4. Transmission electron micrograph of sample particles from the synthetic akaganeite (βFeOOH) particle system.

Frattini (1985). Table 1 summarizes the physical and optical properties of these suspensions. The optical properties were estimated from the available literature. The lower-aspect-ratio system (Wyoming bentonite, average aspect ratio 0.45, or reciprocal 2.22) was generated from commercially available, powdered montmorillonite clays. The more anisometric akaganeite system (β phase of FeOOH, average aspect ratio 6.3) was synthesised by acidic hydrolysis of ferric chloride using a procedure similar to that of Matijevic & Scheiner (1978). Note that the linear-dichroism method makes possible the use of exceedingly dilute colloidal systems (hydrodynamic volume fractions of order 5×10^{-4}).

The physical dimensions of both particle samples were investigated using electron microscopy. Figures 3 and 4 show typical electron micrographs of the bentonite and βFeOOH systems, respectively. The histograms of the particle size and shape distributions derived from examination of many such micrographs are shown in figures 5 and 6 for the bentonite and βFeOOH particles respectively. Despite thorough agitation of the aqueous precursor fluids used to make the bentonite suspensions, these samples still exhibited aggregation which resulted in the high size polydipersity (the ratio of the standard deviation to the mean in the observed size distribution) reported in table 1. On the other hand, the synthetic βFeOOH showed significantly lower size polydispersity, largely due to the synthetic procedure. Great care was taken to avoid particle aggregation, and a large number of micrographs made from very dilute mother liquors indicated the presence of single βFeOOH particles almost exclusively. In §6, effects of polydispersity in particle size are reported for the relaxation in χ by comparing the behaviour of the bentonite and βFeOOH systems following sudden cessation of steady shear.

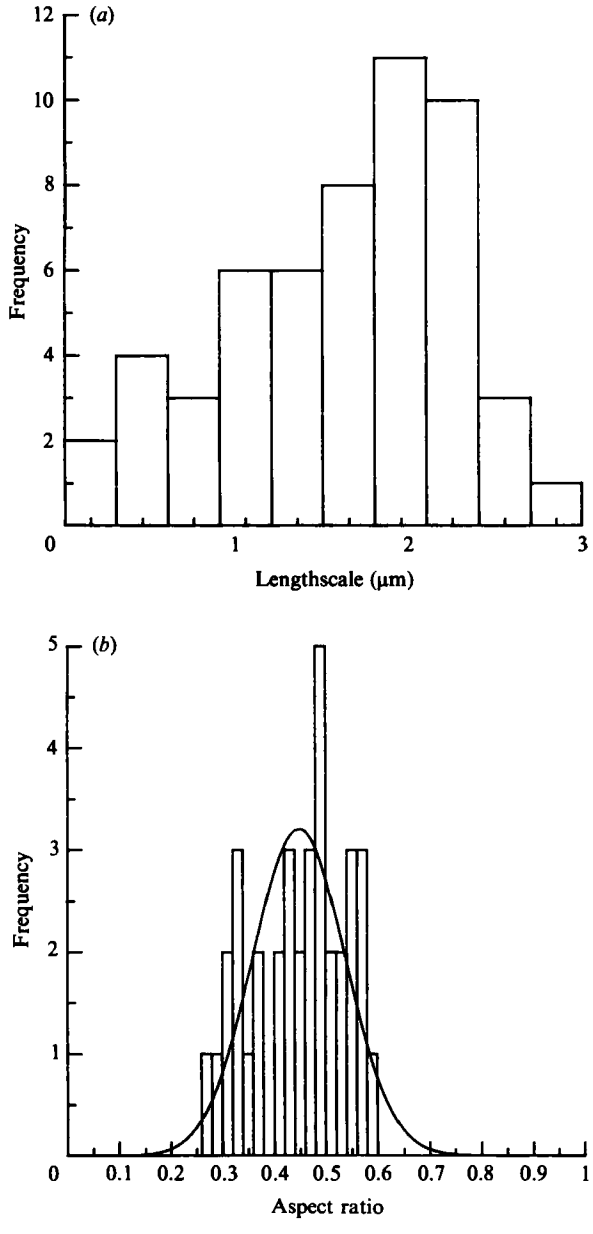

FIGURE 5: Histograms of (*a*) the largest particle dimension and (*b*) the aspect ratio for the bentonite system. Solid curves are fitted Gaussian distributions.

The bentonite and βFeOOH systems are well suited to the study of the weak-Brownian-motion problem during the start-up of simple shear since both the uniformly weak and intermediate regions of rotary diffusion strength are accessible. At the shear rates employed in this work (corresponding to Pe in the range of 20–200), the average bentonite particle falls within the uniformly weak region while the average synthetic akaganeite rod lies in the intermediate regime. In addition, electron

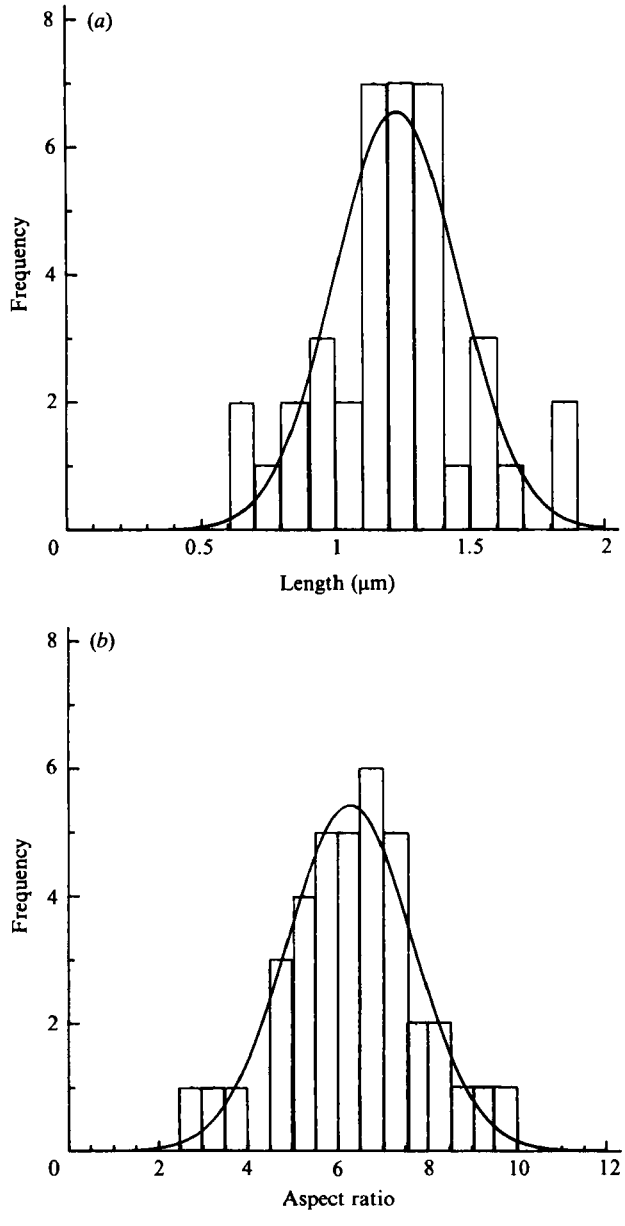

FIGURE 6. Histograms of (*a*) the largest particle dimension and (*b*) the aspect ratio for the βFeOOH system. Solid curves are fitted Gaussian distributions.

microscopy indicated that both systems were approximately equal in aspect-ratio polydispersity. The phase mixing in experimental observables which results from aspect-ratio dispersion, therefore, should not adversely affect a comparison of the data in the two regimes since it is a strong function of the breadth of the aspect-ratio distribution.

3. Second-moment closure

In order to interpret the data presented in §4 and §5, the time evolution of $\langle \boldsymbol{u}\,\boldsymbol{u}\rangle$ following the sudden inception of simple shear with weak Brownian motion is required. In this section, we examine this calculation for a dilute suspension of spheroids which is monodispersed in size and shape. The suspension is hydrodynamically dilute: hence, the particle distribution is translationally invariant. We therefore consider only the orientation distribution of the major axis of the particle.

The orientation distribution function is known in closed form only in the limit of no rotary diffusion ($Pe\to\infty$). Okagawa *et al.* (1973) calculate it directly from the solution of the Jeffery problem with an initially random orientation state:

$$\Psi_\infty = \frac{1}{4\pi[\cos^2\theta + A^2\sin^2\theta]^{\frac{3}{2}}}, \tag{2}$$

where

$$A^2 = A_1\sin^2\phi + \tfrac{1}{2}A_2\sin 2\phi + A_3\cos^2\phi, \tag{3}$$

$$A_1 = \frac{1}{2}\left[1 + r^{-2} + (1-r^{-2})\cos\frac{4\pi t}{T}\right],$$

$$A_2 = (r^{-1}-r)\sin\frac{4\pi t}{T},$$

$$A_3 = \frac{1}{2}\left[1 + r^2 + (1-r^2)\cos\frac{4\pi t}{T}\right],$$

and

$$T = 2\pi(r+r^{-1})/\dot\gamma. \tag{4}$$

Ψ_∞ is normalized on the unit sphere and oscillates with a period of one half the Jeffery period, $\frac{1}{2}T$, as a result of the fore and aft symmetry of the particles. In addition, prolate and oblate particles behave identically under the transformation $r\to 1/r$, $\phi\to\phi+\frac{1}{2}\pi$. Thus, for convenience, we adopt the convention of reporting χ in one quadrant only, $[\frac{1}{4}\pi,\frac{1}{4}\pi]$, with the understanding that the principal axis of an oblate particle would lie orthogonal to the reported direction. The second moment in the absence of Brownian motion is simply

$$\langle \boldsymbol{u}\,\boldsymbol{u}\rangle_\infty = \int_0^{2\pi}\int_0^{\pi} \boldsymbol{u}\boldsymbol{u}\Psi_\infty \sin\theta\,\mathrm{d}\theta\,\mathrm{d}\phi. \tag{5}$$

In order to determine the solution for $\langle \boldsymbol{u}\,\boldsymbol{u}\rangle$ in the presence of weak Brownian motion, we adopt the procedure of solving the second moment evolution equation directly as opposed to attempting to evaluate Ψ first. This is a common technique used in many similar problems. This procedure also affords the most convenient way of incorporating particle size and aspect-ratio dispersion into the data analysis of §§4 and 5. The dynamic equation for $\langle \boldsymbol{u}\,\boldsymbol{u}\rangle$ in a two-dimensional linear flow is developed by appropriate integration of the Fokker–Planck equation describing the time evolution of Ψ (Hinch & Leal 1976):

$$\left[\frac{\mathrm{D}}{\mathrm{D}t} + 6D_{\mathrm{r}}\right][\langle \boldsymbol{u}\,\boldsymbol{u}\rangle - \tfrac{1}{3}\boldsymbol{\delta}] - \boldsymbol{\Omega}\cdot\langle \boldsymbol{u}\,\boldsymbol{u}\rangle - \langle \boldsymbol{u}\,\boldsymbol{u}\rangle\cdot\boldsymbol{\Omega}^{\mathrm{T}}$$
$$-\frac{r^2-1}{r^2+1}[\boldsymbol{E}\cdot\langle \boldsymbol{u}\,\boldsymbol{u}\rangle + \langle \boldsymbol{u}\,\boldsymbol{u}\rangle\cdot\boldsymbol{E} - 2\langle \boldsymbol{u}\,\boldsymbol{u}\,\boldsymbol{u}\,\boldsymbol{u}\rangle : \boldsymbol{E}] = 0, \tag{6}$$

where $\boldsymbol{E}$ is the rate-of-strain tensor and $\boldsymbol{\Omega}$ is the vorticity tensor of the imposed flow and where D_{r} is the Stokes–Einstein rotory diffusivity for a spheroid of specified size and aspect ratio. Equation (6) typifies the closure problem inherent to many

stochastic systems: the equation for $\langle \boldsymbol{u}\,\boldsymbol{u}\rangle$ depends explicitly on the unknown higher moment $\langle \boldsymbol{u}\,\boldsymbol{u}\,\boldsymbol{u}\,\boldsymbol{u}\rangle$. As Hinch & Leal (1976) point out, a finite, closed system of equations for a finite set of moments does not exist. In order to proceed with the solution of (6), a functional relationship between the second and fourth moments must be specified *a priori*. The general solution for the distribution function, however, is also unknown. The closure relation will therefore be approximate at best. It is one of the purposes of this work to investigate experimentally the validity of two such closure approximations in terms of their utility and accuracy in describing the suspension mechanics. The nature of the decoupling approximation not only affects the calculation of the average particle orientation direction and degree of alignment but also influences predictions of the stress state in the suspension since the particle contribution to the stress depends upon both the second and the fourth moments.

We first consider the so called pre-averaging approximation (PA) where the left most dyadic in the fourth moment is replaced by its average value:

$$\langle \boldsymbol{u}\,\boldsymbol{u}\,\boldsymbol{u}\,\boldsymbol{u}\rangle : \boldsymbol{E} \approx \langle \boldsymbol{u}\,\boldsymbol{u}\rangle\langle \boldsymbol{u}\,\boldsymbol{u}\rangle : \boldsymbol{E}. \tag{7}$$

This closure deserves attention for its simplicity and also for its preponderance of use in many similar problems. The PA form is completely *ad hoc*, however, for the case of shear flow. in fact, for the weak-Brownian-motion problem, it becomes asymptotic only in the limit of large Pe, highly extensional flows where the distribution function is strongly peaked about a single director. One may anticipate difficulty in describing the particle orientation state via (7), then, when the imposed flow contains more than a small amount of vorticity. Bird, Warner & Evans (1971), for example, calculate the relative viscosity enhancement and the primary normal stress coefficient of a suspension of rigid dumb-bells subjected to steady simple shear with Brownian motion. These authors find that while the PA calculation exhibits the correct overall qualitative features, it generally is in poor quantitative agreement with the numerical results of Stewart & Sørensen (1972).

As an alternative to (7), we consider the leading-order closure suggested by Hinch & Leal (1975, 1976). These authors propose an interpolation scheme whereby the strong- and weak-flow asymptotic forms for the fourth moment in a two-dimensional linear flow are matched to provide a composite which would hopefully represent an accurate closure over the entire range of Péclet numbers. Their leading-order composite (HL) takes the following form:

$$\langle \boldsymbol{u}\,\boldsymbol{u}\,\boldsymbol{u}\,\boldsymbol{u}\rangle : \boldsymbol{E} \approx \tfrac{1}{5}[6\langle \boldsymbol{u}\,\boldsymbol{u}\rangle \cdot \boldsymbol{E} \cdot \langle \boldsymbol{u}\,\boldsymbol{u}\rangle - \langle \boldsymbol{u}\,\boldsymbol{u}\rangle\,\langle \boldsymbol{u}\,\boldsymbol{u}\rangle : \boldsymbol{E} - 2\delta\langle \boldsymbol{u}\,\boldsymbol{u}\rangle^2 : \boldsymbol{E} + 2\delta\langle \boldsymbol{u}\,\boldsymbol{u}\rangle : \boldsymbol{E}]. \tag{8}$$

As Hinch & Leal point out, the strong-flow limit of (8) is simply an expression equivalent to (7) and therefore (8) is also *ad hoc* in the case of shear flow at high Pe. Equation (8), however, obtains the correct limiting form as $Pe \to 0$ in shear flow. As a result, the HL approximate may provide a better description of the orientation state induced in the suspension at intermediate values of Pe than the PA closure. Hinch & Leal (1976) compare the steady state intrinsic viscosity and normal stress differences calculated using (8) with exact results (Scheraga 1955; Scheraga *et al* 1951) for spheroids with aspect ratio 5 and 25 in simple shear with $Pe < 20$. The HL closure produces a good approximation to the exact intrinsic viscosity and first normal stress difference at the lower aspect ratio. First normal stress agreement at the higher aspect ratio is significantly reduced, however, with an error approaching 40 % near $Pe = 20$. The second normal stress shows equally poor agreement for both aspect ratio particles. These authors also develop a higher-order interpolation which significantly increases the accuracy of (8) in extensional fields. For simple shear, however, it

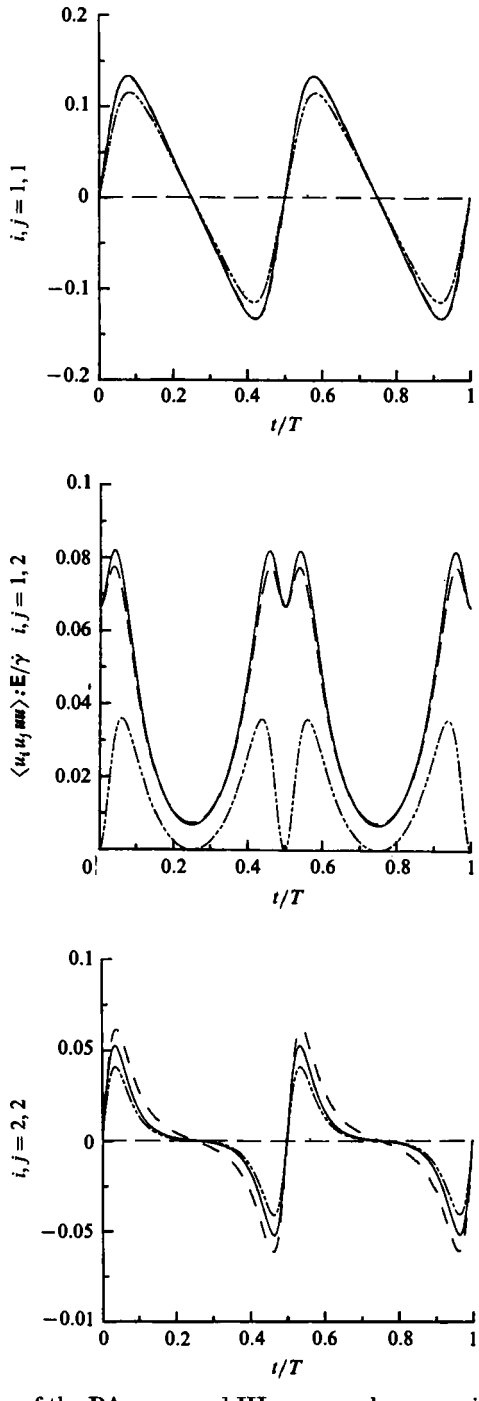

FIGURE 7. Comparison of the PA, – – –, and HL, — · —, closures using exact values of $\langle \boldsymbol{u}\,\boldsymbol{u} \rangle$ to the exact values, ——, of $\langle u_i u_j \boldsymbol{u}\,\boldsymbol{u} \rangle : \boldsymbol{E}/\dot{\gamma}$ in the absence of Brownian motion for $r = 5$. (i,j): flow term $(1,1)$, gradient term $(2,2)$, cross term $(1,2)$.

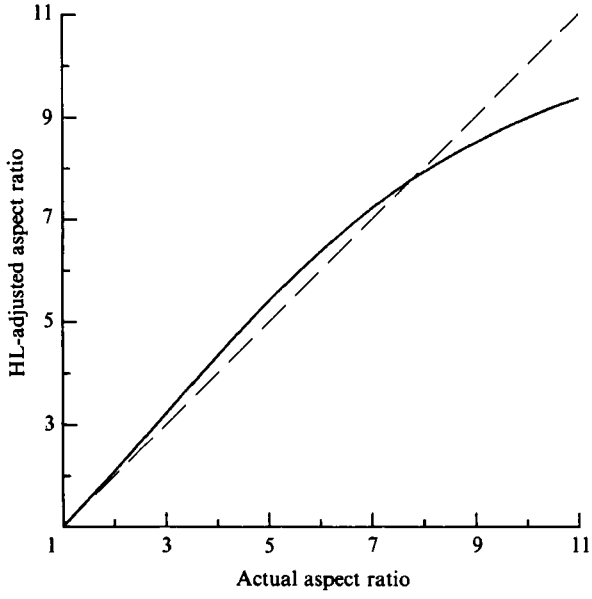

FIGURE 8. The adjusted aspect ratio, r_a, as a function of the actual particle aspect ratio, r. The solution of the moment equation with HL closure for a particle of aspect ratio r_a in the absence of Brownian motion oscillates with the Jeffery period of a particle of aspect ratio r. $Pe = \infty$.

improves the second normal stress prediction while decreasing the accuracy of the lower aspect ratio first normal stress calculation. Since the experimental method employed in this work is sensitive only to changes in the plane of shear, the higher-order interpolation does not merit further attention here.

It is of interest to compare (7) and (8) in the limit of $Pe \to \infty$ where the distribution function Ψ_∞ is known in closed form. Figure 7 illustrates the relative accuracy of (7) and (8) in this limit. The exact time evolution of the relevant components of $\langle u_i u_j \boldsymbol{u}\boldsymbol{u}\rangle : E/\dot{\gamma}$ (that is, the flow term $\{i,j\} = \{1,1\}$, the gradient term $\{i,j\} = \{2,2\}$, and the cross-term in the plane of shear $\{i,j\} = \{1,2\}$) was calculated directly by integration of (2) for a suspension containing particles of aspect ratio 5 subjected to the sudden inception of simple shear from rest. The plots generated from (7) and (8) for these terms facilitate a best case comparison at $Pe \to \infty$ in that the closure approximations were evaluated using the exact value of $\langle \boldsymbol{u}\boldsymbol{u}\rangle$ from (5). The HL closure provides an acceptable estimate of all three terms, with essentially perfect agreement occurring in the $\{1,1\}$ term. On the other hand, the PA closure is acceptable for the $\{1,1\}$ and $\{2,2\}$ terms but fails miserably in the cross-term plot. In particular, the PA calculation obtains the wrong initial condition for this moment. From consideration of the initial-value scheme used to numerically solve (6) in simple shear, it becomes apparent that this error causes a large overprediction in the initial rate of change of $\langle u_1 u_2\rangle$ which, in turn, results generally in an overestimate of the degree of alignment as calculated from (1). It is not surprising that the HL closure obtains the correct initial condition, though, since the random distribution associated with the rest state is identical, to leading order, to the particle orientation distribution in the weak-flow limit. Analogous conclusions apply to the same calculations done for particles of aspect ratio 2 and 10. In addition, it is worth pointing out that the higher-order interpolation suggested by Hinch & Leal (1976) actually fares worse than (8) in this calculation at all three aspect ratios (Frattini 1985).

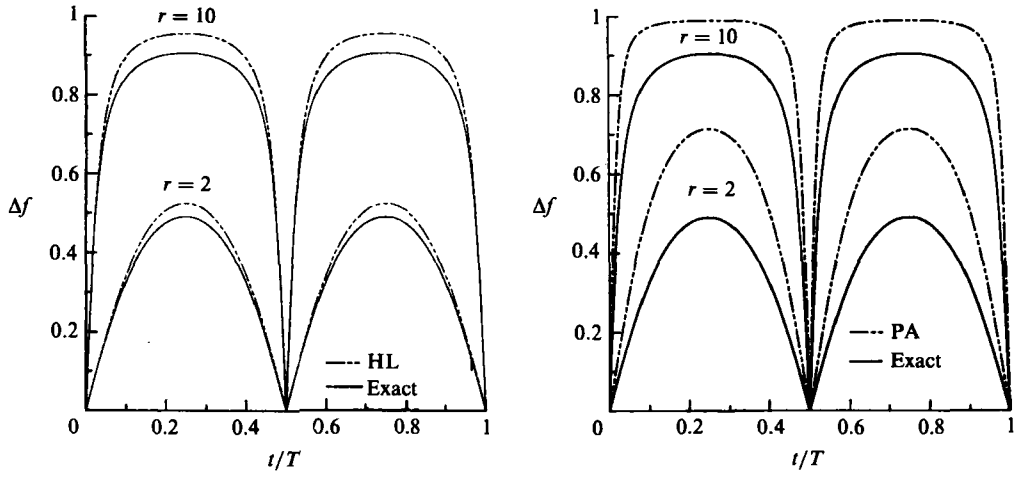

FIGURE 9. Comparison of the exact degree of alignment to that predicted using the HL and PA closures in the absence of Brownian motion for particles of aspect ratio 2 and 10. $Pe = \infty$.

While the PA closure appears to be far inferior to the HL approximate for simple shear flow at both the high and low Pe limits, direct integration of (6) using (8) in the limit of very large Pe uncovers one difficulty specific to the HL closure. This procedure results in an error in the predicted Jeffery period which did not appear in figure 7 (where (5) was used for the second moment). Hinch & Leal (1976) noted that the period of the viscosity and normal stresses for a particle system of aspect ratio 5 was too small by 7%. The relative error in the predicted period actually depends upon r and diverges as r becomes large. Figure 8 illustrates this effect. We plot the adjusted value of the aspect ratio, r_a, versus the actual particle aspect ratio, r, where r_a is that value of the aspect ratio for which the large Pe integration of (6) using (8) results in $\langle \boldsymbol{u}\,\boldsymbol{u} \rangle$ which oscillate with the Jeffery period of a particle of aspect ratio r. Figure 8 suggests that r_a differs only minimally from r for values of $r < 10$. Identical results hold for oblate particle under the transformation $r \to 1/r$. The discrepancy induced in the period by the HL procedure will unfortunately skew the HL models of the data toward unrealistic periods as a result of the aspect-ratio dependence to the error in the predicted period coupled with the experimentally observed dispersion in particle shape. Even accounting for dispersion in particle shape, at least 95% of the particles employed in the experimental portion of this work fall within the range r (or $1/r$) less than 10. In order to avoid this error when comparing HL calculations to experimental data, therefore, we adopt an arbitrary but reasonable procedure of adjusting the actual particle aspect ratio to r_a via figure 8 prior to performing the HL data fitting. Hence, both the HL and PA predictions of the data will obtain the correct period in the high Pe limit. Figures 9 and 10 illustrate respectively the degree of alignment and the orientation angle calculated from (1) using this procedure at infinite Péclet number for an actual particle aspect ratio of 2 and 10. The exact calculations (using (5)) are compared to the results of integrating (6) using the HL closure with period adjustment and using the PA approximation (7). The overprediction of the degree of alignment is much worse in the PA case. For χ, the HL procedure proposed here is in excellent agreement with the exact calculation, and the PA result is numerically indistinguishable from the exact curve. This strong agreement perhaps is not as highly indicative of the validity

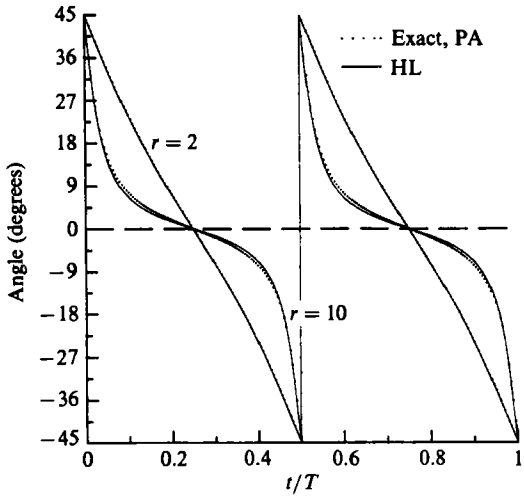

FIGURE 10. Comparison of the exact orientation angle to that predicted using the HL and PA closures in the absence of Brownian motion for particles of aspect ratio 2 and 10. $Pe = \infty$.

of the suggested closures as one might initially be led to believe, particularly where the bulk rheological properties of the suspension are concerned. Ψ_∞, for example, possesses the peculiar feature that χ calculated from the near sphere limit (to $O[(\Lambda^2-1)^2]$) with values of r far outside the range $|r-1| \ll 1$ is actually quantitatively close to the exact result given by (5) (Frattini 1985). In addition, the suspension viscosity and normal stress differences may be expected to be much more sensitive to the degree of particle alignment about a given direction than to the actual orientation of the alignment direction.

4. Data in the uniformly weak regime

Figure 11 shows, in composite form, the magnitude of the dichroism and orientation angle χ measured for the bentonite system subjected to simple shear flow at three Péclet numbers: 36, 72 and 144. Recall that bentonite is a low-aspect-ratio particle. The large majority of the particles in the suspension fall within the uniformly weak regime of Brownian motion at these flow strengths. The data exhibited a reasonable amount of oscillation prior to obtaining a steady state. In fact, the apparent period and rate of damping of the highest-Pe data set was within a few per cent of that expected for this suspension in the absence of Brownian motion; that is, when damping would be due exclusively to the phase-mixing effect resulting from particle-shape dispersion. As Pe decreased, the magnitude of the steady-state dichroism decreased and the relative damping in the dichroism oscillations increased. In the absence of Brownian motion, dispersion in aspect ratio is expected to cause the observed value of χ to phase mix toward zero degrees. As Pe decreased, the steady-state angle increased above zero with the damping in the oscillations in χ increasing as well. Shearing this suspension at Pe of order 10^3 resulted in a steady state χ of zero degrees. There was little discernable effect of Pe on the apparent period of the oscillations in the data at the flow strengths attained here.

The qualitative features of the data presented in figure 11 are in general agreement with what might be expected from previous theoretical treatments of the weak-

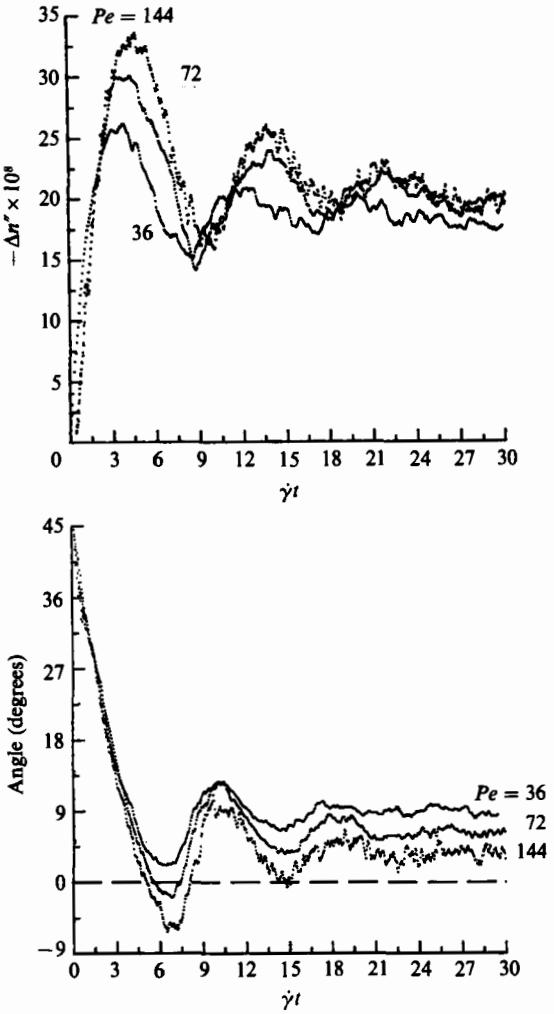

FIGURE 11. Bentonite data in the uniformly weak regime of Brownian motion with imposed simple shear flow; magnitude of the linear dichroism and average orientation angle as a function of total strain at three Péclet numbers: 36, 72, 144.

Brownian-motion problem. Before presenting a more quantitative comparison to the models of §3, several remarks concerning the data analysis in general are in order. First of all, it is essential to account for the experimentally observed polydispersity in particle size and aspect ratio. The moments $\langle \boldsymbol{u}\,\boldsymbol{u} \rangle$ calculated by the methods of §3 are therefore averaged over least-squares best-fit Gaussian distributions in size and shape (with mean and variance given in table 1) prior to calculating the orientation angle and degree of alignment by (1). While the use of a normal distribution function to describe shape dispersion has a precedent in the literature (Cerda *et al.* 1981), it may seem unorthodox for describing size dispersion. In the case of the synthetic βFeOOH, the length of the rod depends upon reaction time which, in turn, is determined by the distribution in crystallization initiation events. The latter may reasonably be assumed to be Gaussian. On the other hand, the electron micrographs of the bentonite do indicate a non-negligible fraction of very small particles which

would be better accounted for by a typical lognormal distribution. As a result of the strong length dependence of Pe, however, this fraction obtains an effective Péclet number much less than one and thus contributes nothing to the overall size average of $\langle \boldsymbol{u}\,\boldsymbol{u} \rangle$. A normal distribution provides a better fit of the remaining particles and is therefore used to describe the bentonite size dispersion.

Secondly, as (1) implies, models of the data are a one-parameter fit. The prediction of the orientation angle, however, has no adjustable parameters. In addition, the one unknown, $\Delta n''_{\max}$, is determined for each suspension independent of the closure approximation used to model the data. In this sense, the data represent quite a stringent test of the PA and HL closures. Since both the particle-aspect-ratio distributions and Ψ_∞ are known, $\Delta n''_{\max}$ can easily be determined by comparing the steady-state (fully phase mixed) dichroism measured at high shear rate to the exact calculation of the degree of alignment in this limit. In this way, $\Delta n''_{\max}$ was found to be 7.49×10^{-7} for the bentonite suspension and 2.06×10^{-7} for the akaganeite suspensions. Of course, this procedure neglects any size dependence of $\Delta n''_{\max}$; that is, we have effectively factored the optical parameters of the scattering problem out of the size integration and have averaged only the orientational component, $\langle \boldsymbol{u}\,\boldsymbol{u} \rangle$, over the size distribution. This procedure is exact in the limit of a Rayleigh particle. In the Rayleigh approximation, conservative dichroism arises solely from the intrinsic optical anisotropy of the scatterer, and therefore $\Delta n''_{\max}$ does not depend explicitly on the physical dimensions of the particle. The bentonite particles, however, are typically not small compared to the wavelength of the light source. One might argue that a polycrystalline system such as bentonite would not possess sufficient intrinsic optical anisotropy to fully dominate the scattering effects of particle form. The bentonite data presented below, however, suggest that the above procedure for determining $\Delta n''_{\max}$ does not impose significant restriction on the evaluation of the accuracy of the models used to interpret this data. In addition, the first correction to the Rayleigh treatment for the effect of particle size can be calculated using the Rayleigh–Gans approximation to the light scattering (Frattini 1985). In this treatment, the length dependence of the optical parameters of particles having the size of bentonite is much weaker than the Péclet-number dependence of the orientational portion of the scattering. The βFeOOH particles used in this study, on the other hand, exhibit an intrinsic optical anisotropy which is an order of magnitude larger than that of the bentonite system and which fully dominates the scattering mechanism. In addition, the size of these particles is the order of the wavelength of the light source. Applying the Rayleigh limit in estimating $\Delta n''_{\max}$, therefore, would not be expected to cause significant error in the interpretation on the data from either the bentonite or the βFeOOH particle system.

Finally, the values of the Péclet number reported for the data are those derived from the experimental shear rates and the calculated Stokes–Einstein rotary diffusivity of a spheroid evaluated with the average particle dimensions. As was pointed out previously with respect to the high degree of polydispersity in the size of the bentonite particles, the diffusivity calculated by straightforwardly averaging the Stokes–Einstein result over the measured distributions in the particle dimensions would skew the reported Péclet number unrealistically toward the smaller particles. The method of calculating the reported Pe here, however, provides an adequate basis from which the bentonite and the βFeOOH systems, which differed widely in size polydispersity, may be compared. In addition, the diffusivity calculated for the average particle agreed well with the long time relaxation rate of the dichroism for these suspensions.

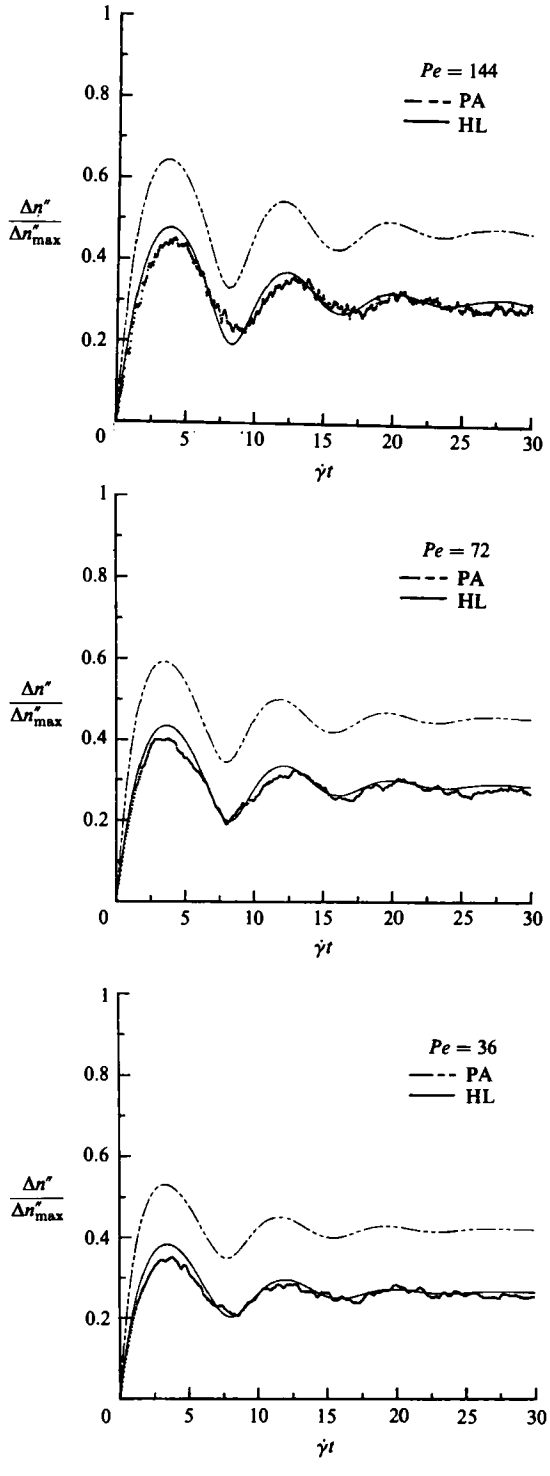

FIGURE 12. Comparison of the degree of alignment calculated from the bentonite data of figure 11 to that calculated using the PA and the HL closure approximations.

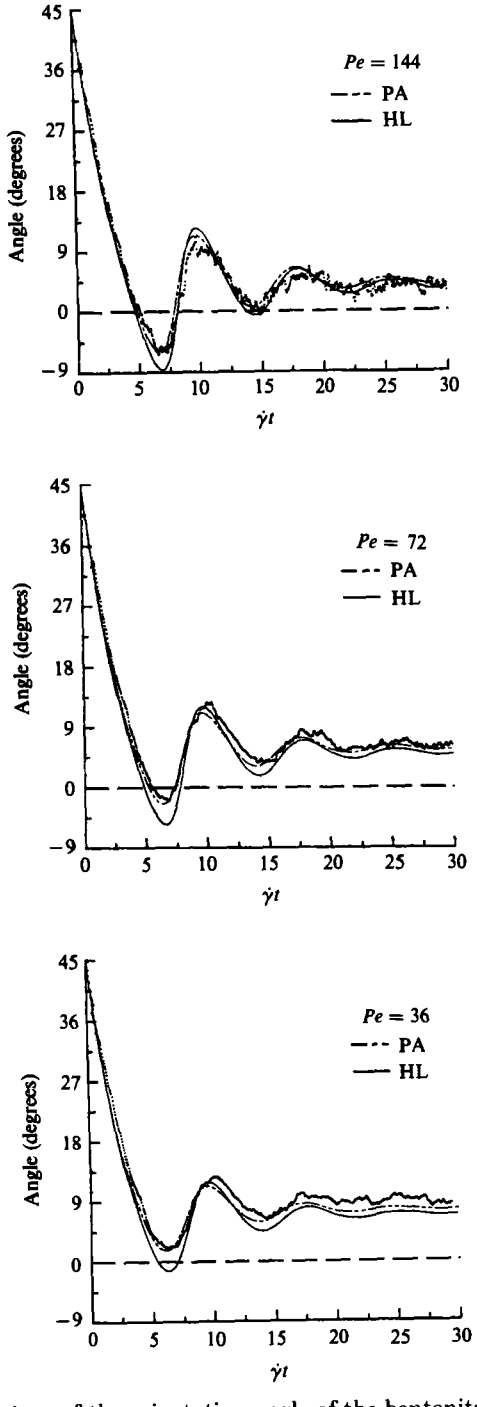

FIGURE 13. Comparison of the orientation angle of the bentonite data of figure 11 to that calculated using the PA and the HL closure approximations.

Figure 12 shows the degree of alignment implied by the data of figure 11 compared with that calculated using the PA and HL closures. The HL closure does an excellent job of modelling the data over the full range of Pe while the PA approximation drastically overpredicts the degree of alignment for all time. We should point out, however, that the PA closure predicts the correct period of the data given only the observed aspect-ratio distribution while the HL result would not have attained such agreement had the aspect ratio used in the calculation not been adjusted as described in §3. Still, the HL agreement seems remarkable given the relatively uncharacterized nature of the bentonite particles. Figure 13 illustrates the comparison of the data and calculations in the case of the orientation angle. Recall that there are no adjustable parameters here. Both closures provide acceptable models at the larger Pe but underpredict the angle (that is, underestimate the magnitude of the Brownian effects) as Pe decreases. In addition, the magnitude of the oscillations in the HL calculation seems slightly greater than that warranted by the data. Overall, however, the HL closure appears superior to the PA closure in the uniformly-weak-Brownian-motion regime.

5. Data in the intermediate regime

Figure 14 summarizes the orientation and degree of alignment data taken on the βFeOOH system subjected to the sudden inception of simple shear at Péclet numbers ranging from 23 to 187. At these flow strengths, the large majority of the particles in the sample fell within the intermediate regime of weak Brownian motion, $Pe^{-1} \ll 1$ and $Pe < (r+1/r)^3$. The overall qualitative features of these data as a function of Pe were similar to those exhibited by the bentonite system over a similar range of Pe. Two differences, however, were evident which qualitatively illustrate the effect of aspect ratio on the strength of the Brownian diffusion at a given Pe. Note first that even though the particle aspect-ratio dispersion, and therefore its resultant phase-mixing effect, are almost identical for the two particle systems, the relative damping of the oscillations in the data was significantly enhanced for the higher-aspect-ratio system. Since the shear rates for the bentonite experiments were of the same order as those for the βFeOOH experiments, one might argue that this effect was merely a result of the fact that the Jeffery period of the βFeOOH was longer in real time than that of the bentonite. While the randomizing effects of diffusion will of course accumulate with time, closer inspection of the data suggests the presence of an additional damping mechanism. The period of the oscillation in the βFeOOH data was a more strongly decreasing function of Pe than in the bentonite data. This difference is particularly evident in the time of the first minimum in the average-orientation-angle data. Recall that the aspect ratio of these particle systems was somewhat polydispersed; the βFeOOH sample could have contained particles with an aspect ratio as high as 10. Since the Jeffery period increases with aspect ratio, a comparison of the Pe dependence of the period of the data from figures 11 and 14 suggests that, as Pe decreased, the orientational oscillations of higher-aspect-ratio particles are damped out more quickly than those of less anisometric particles. This observation is consistent with the concept of an aspect-ratio dependence to the local Péclet number in the intermediate-strength regime of weak Brownian motion.

The data of figure 14 are compared to the PA and HL model predictions for the degree of alignment and for the average orientation direction in figures 15(a, b) and 16(a, b) respectively. Recall that there are no adjustable parameters in the orientation

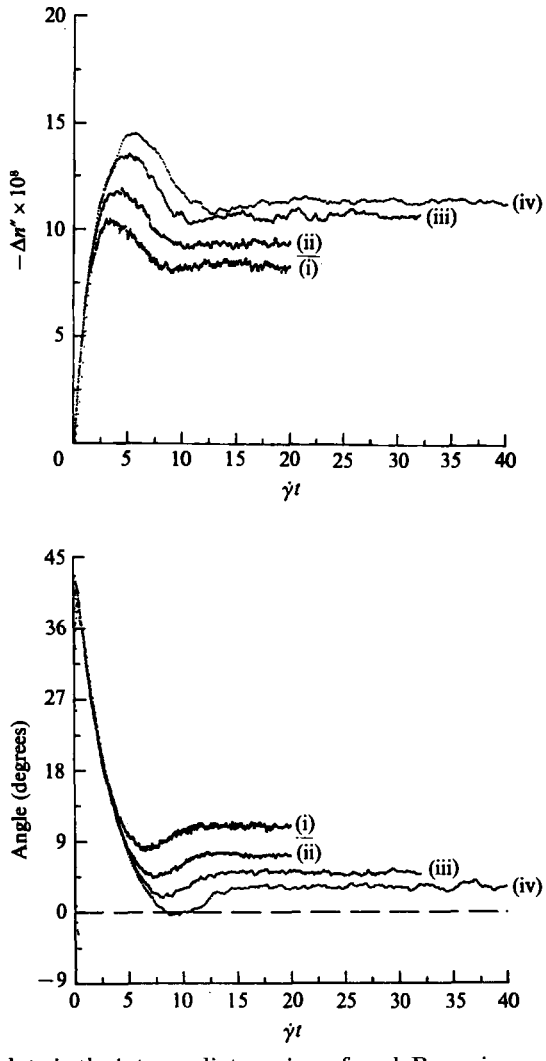

FIGURE 14. βFeOOH data in the intermediate regime of weak Brownian motion with imposed simple shear flow; magnitude of the linear dichroism and average orientation angle as a function of total strain at four Péclet numbers: (i) 23, (ii) 47, (iii) 94, (iv) 187.

angle calculations, and that the only adjustable parameter in the degree of alignment fit, $\Delta n''_{\max}$, is chosen independently of the particular closure approximation employed in the model. Of course, the larger the aspect ratio of the particle the greater the overall degree of alignment should be when Brownian motion is absent. One might therefore intuitively expect that (7), or equivalently the strong-flow asymptotic form of (8), would provide a more accurate approximation for a suspension of larger rather than smaller aspect ratio particles sheared at high Pe. While this trend would most likely hold true if the rotary diffusion were uniformly weak, the data in the intermediate regime strongly indicate that this intuitive approach is misleading. This general feature of the fully time-dependent data concurs with the aspect-ratio dependence of the steady state viscometric functions calculated previously using (8) at $Pe < 20$ (Hinch & Leal 1976).

Figures 15(*a*, *b*) and 16(*a*, *b*) suggest that the PA closure is a poor approximation to the orientation state induced in a sheared suspension under intermediately-weak-Brownian-motion conditions. The PA closure model drastically overpredicts the degree of alignment at all times for the range of *Pe* under study. In fact, the steady-state values are pinned so closely to unity that the relative overshoot which is predicted by the model markedly understates the values observed from the data. The PA model also tends to strongly overpredict the average orientation angle induced in the suspension, with the discrepancy between theory and data increasing with decreasing *Pe* to the point that the predicted relative undershoot becomes negligibly small. Since lower Péclet numbers generally imply higher induced angles, the orientation-angle data in figures 16(*a*, *b*) suggest that the PA approximation overestimates the strength of rotary diffusion effects in the singular regime; that is, overestimates the aspect-ratio enhancement of diffusion effects corresponding to locally strong perturbations to the Jeffery motion. At first glance, the degree-of-alignment calculation may seem to contradict this statement. Recall, however, that even in the absence of Brownian motion, the PA closure markedly overestimates the exact degree of alignment (figure 9) while the angle is accurately predicted in this limit (figure 10). In fact, it seems plausible that precisely this effect precipitates the overprediction of the average orientation-angle data; the very large overestimates of the degree of alignment imply large overestimates of the orientational gradients in the singular region of configuration space which in turn manifest themselves as the larger orientation angles indicative of stronger Brownian motion effects.

The HL closure is far superior to the PA closure for interpreting the data in the intermediate regime but falls short of attaining accuracy equivalent to that of the HL calculations in the uniformly weak regime of Brownian motion. The HL results of figures 15(*a*, *b*) and 16(*a*, *b*) suffer on two counts. We believe that both points, however, stem from the same source; namely, the inability of (8) to describe the intermediate shear form of the closure in the singular regime where the overall Péclet number but not the local Péclet number, corresponding to the particle alignment region, remains large. First, the overall magnitude of the HL degree of alignment systematically overstates the data over the full range of *Pe* studied. The initial overshoot as a percentage of the steady-state value is also overstated at the higher end of the *Pe* range. Secondly, the apparent period of the HL calculations consistently overestimates that of the data. Both of these observations lend support to the hypothesis that (8) underestimates the aspect-ratio enhancement of the local rotary diffusion effects in the singular region; that is, the higher-aspect-ratio particles in the sample contribute more to the orientation state of the suspension in the HL calculation than is warranted by the data. Thus, the physical model employed to develop the strong flow limit in the HL closure procedure (that is, a distribution function sharply peaked about a single director, which does not obtain the correct high shear asymptotic form) results in a less accurate interpolation for shear flow in the intermediate regime than for shear flow in the uniformly weak regime of weak Brownian motion.

The comparison of the HL angle calculations to the data (figures 16*a*, *b*) support the conclusion drawn from the degree of alignment analysis. Note, however, that the agreement between the calculated steady state and the data is closer for the orientation angle than for the degree of alignment. This discrepancy most likely results from the use of the lowest-order approximate to the light scattering from βFeOOH. The extinction angle, a fundamentally geometric quantity, is less sensitive to the choice of approximation for the optical theory than the magnitude of the

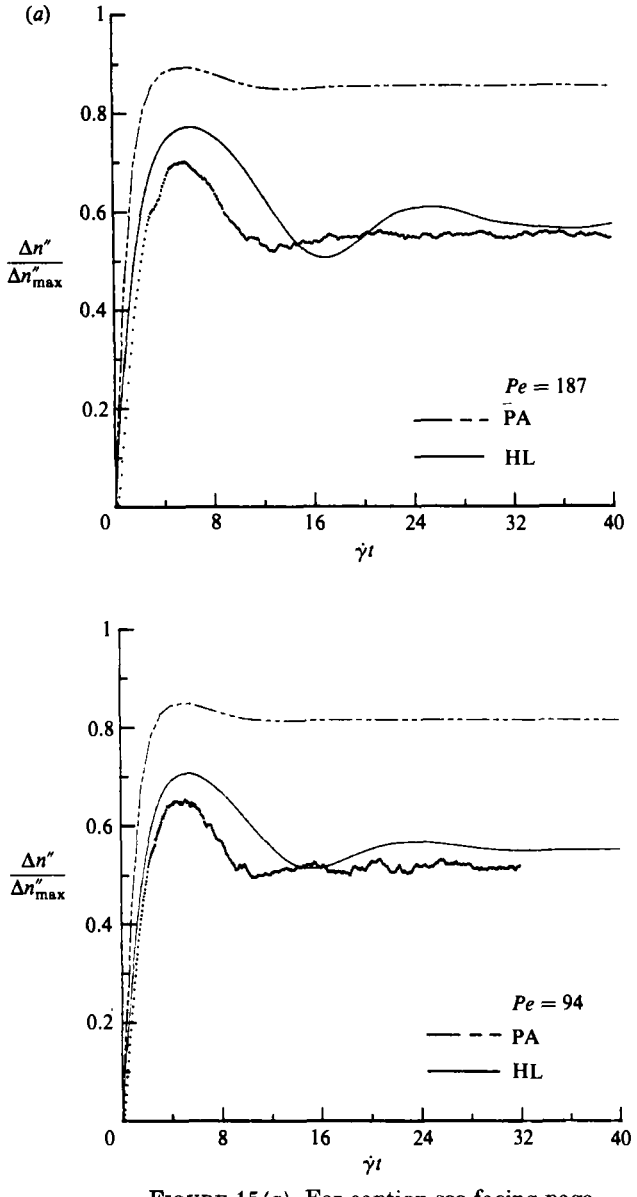

FIGURE 15(a). For caption see facing page.

dichroism. The apparent period and the initial relative overshoot in the degree of alignment calculations are expected to be equally insensitive to the errors inherent to the light-scattering treatment. Note that accuracy of the HL predictions of the angle, the apparent period and the initial relative overshoot in the degree of alignment improves with decreasing Pe. This trend is expected since (8) is asymptotic as $Pe \to 0$, and hence it lends further support to the notion that significant conclusions concerning the fluid mechanics of the particle system can be drawn from rheo-optical data without the necessity of exacting accuracy in the optical treatment. In addition, the qualitative features of the HL calculations shown in figures 15(*a*, *b*) and 16(*a*, *b*), and therefore the conclusions drawn from comparing these calculations with the

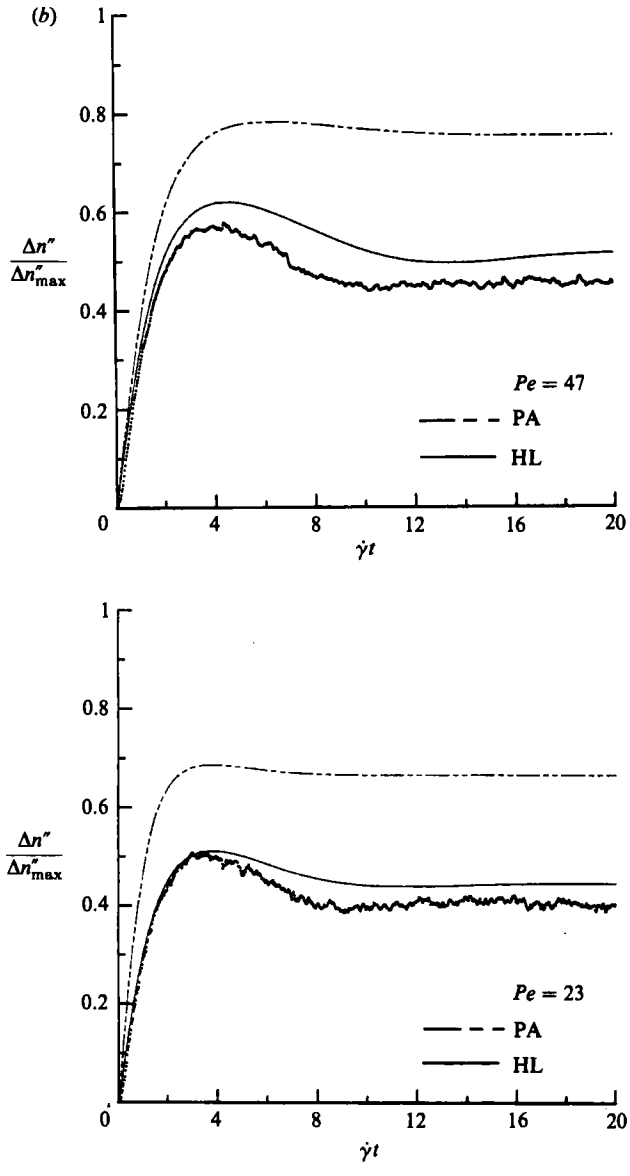

FIGURE 15. Comparison of the degree of alignment calculated from the βFeOOH data of figure 14 to that calculated using the PA and HL closure approximations: (*a*) $Pe = 187, 94$; (*b*) $Pe = 47, 23$.

data, are altered neither by the inclusion of a correction in the diffusivity calculation for the apparent blunt ends of the particles (figure 4) nor by the aspect-ratio-adjustment procedure described in §3.

In summary, then, the particle dynamics of a dilute suspension subjected to the inception of simple shearing flow with weak Brownian motion have been investigated experimentally using a recently developed rheo-optical method based on conservative linear dichroism. This technique affords a complete, time dependent characterization of the flow-induced orientation state in that both the degree of particle alignment and the average alignment direction projected in the shear plane are measured

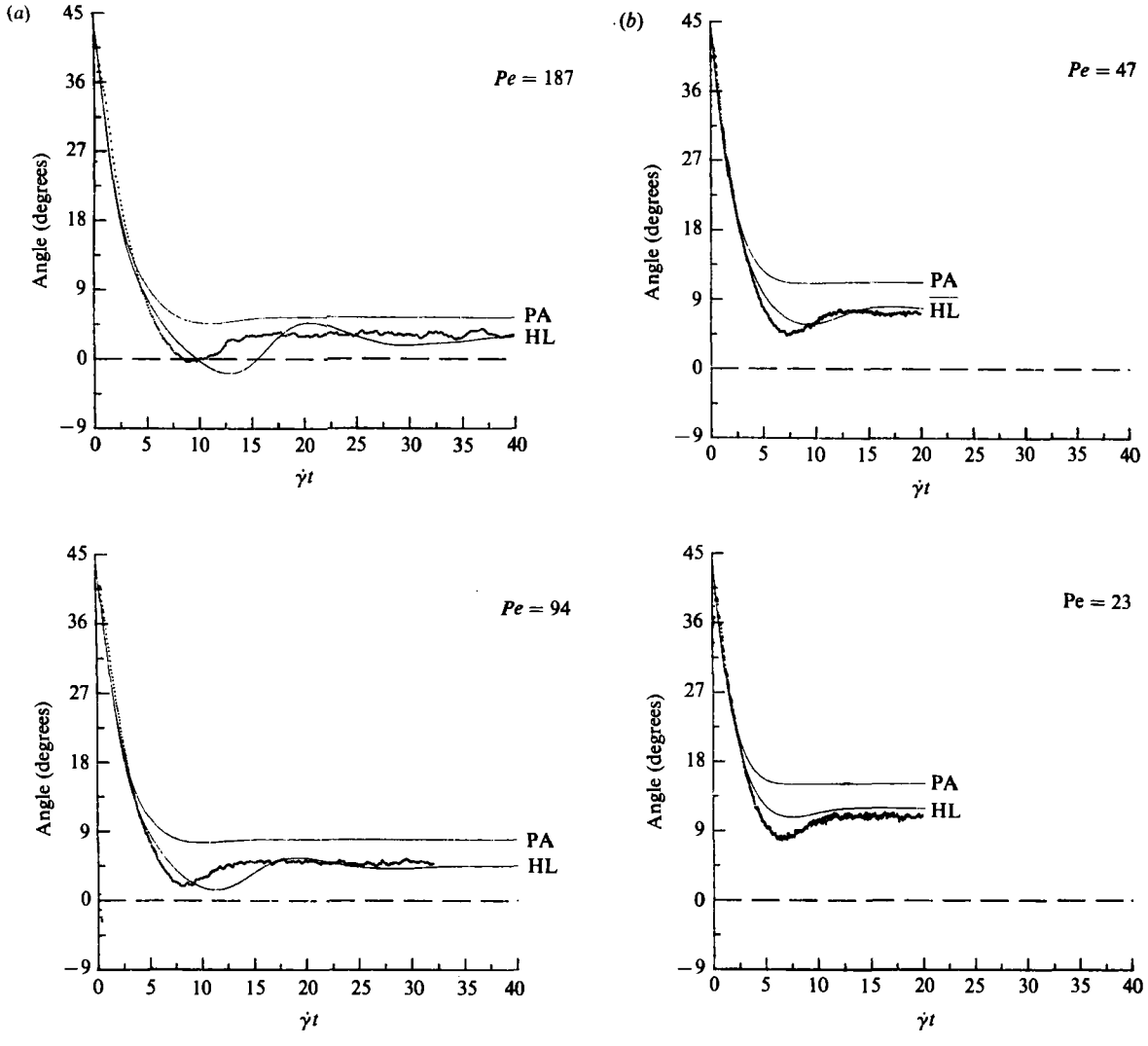

FIGURE 16. Comparison of the orientation angle of the βFeOOH data of figure 14 to that calculated using the PA and the HL closure approximations: (*a*) $Pe = 187, 94$; (*b*) $Pe = 47, 23$.

simultaneously. The data indicate that the Hinch–Leal closure procedure results in a very accurate model of the particle dynamics in the limit of uniformly weak Brownian motion. In the intermediate regime of weak Brownian motion, this model adequately represents the qualitative features of the data but does not achieve the same quantitative accuracy exhibited in the uniformly weak case. While the data suggest that perhaps a re-examination of the form of the Hinch–Leal closure is in order in this particular regime of intermediate flow strength, the overall success of the closure in modelling the data in this study supports the development of Hinch–Leal type procedures as alternatives to simple pre-averaging methods in similar problems where the nature of the closure approximation strongly affects the accuracy of the model calculations.

As a result of the development of the linear dichroism technique, an experimental

approach to many important and interesting problems in the microdynamics of particulate systems is now feasible. These more fundamental experiments might include, for example, studies of particle suspensions in non-Newtonian liquids, studies of particle–particle interactions, studies of orbit drift due to departures in axisymmetry, studies of structure induced in anisotropic fluids such as liquid crystals, and investigations of the effects of externally imposed fields on suspension dynamics. In addition, the availability of accurate yet tractable modelling procedures extends the utility of the rheo-optical technique employed in this work to more practical areas. For example, the interpretation of experiments using flow fields to probe the particle size and shape distributions of unknown suspensions is invariably complicated by perturbing effects such as Brownian motion. The availability of an appropriate rheo-optical method, such as the dichroism technique, coupled with an accurate modelling procedure, such as the Hinch–Leal method when Brownian motion is uniformly weak, makes possible the study of many important problems in particle characterization.

6. Relaxation after cessation of shear

In this final section, we present experimental results for the suspension relaxation following sudden cessation of simple shear flow at steady state. In particular, the wide disparity in size polydispersity between the bentonite and the synthetic βFeOOH suspensions facilitates an experimental investigation of the effects of polydispersity in the particle lengthscale during relaxation. In addition, the dichroism method used here makes possible the simultaneous observation of the degree of alignment and of the average orientation direction during relaxation.

The initial states of both $\Delta n''$ and χ at the moment of cessation of course depend upon the rotary Péclet number of the imposed flow which in turn is a strong function of particle length. There is little novelty in the effects of size polydispersity on the decay of the magnitude of the dichroism induced by shear at very high Pe. The rate at which the suspension relaxes toward the random state depends upon the lengthscale of the particles and thus multiple modes of dichroism relaxation are expected. The feature of the dichroism relaxation which perhaps is not commonly appreciated is that in the presence of size polydispersity with even quite weak Brownian motion during the flow, the modes of relaxation vary with the Péclet number of the aligning shear. This effect is illustrated in figure 17 where the relaxation of $\Delta n''$ normalized by its value during steady shear is plotted as a function of time following sudden cessation of the flow fields which produced the βFeOOH data of figure 14. Note that at longer times, the slope of the data approached a common value, whereas the initial decay rate increased with increasing Pe. The strength of the flow effectively truncates the microscopically observed size distribution to only those sets of particles whose degree of alignment produces a measurable contribution to the dichroism signal.

The relaxation spectrum of the orientation direction, on the other hand, has heretofore not been studied in detail for suspensions. Consider first a monodispersed suspension. The orientations of all particles randomize at the same rate, and therefore the average projection of the major axis of the particles into the shear plane remains constant during the suspension relaxation independently of the strength of the aligning shear field. Size polydispersity coupled with weak Brownian motion during the flow, however, produce an interesting decay in the orientation direction during relaxation which is shown in figures 18 and 19 for, respectively, the relaxation of the

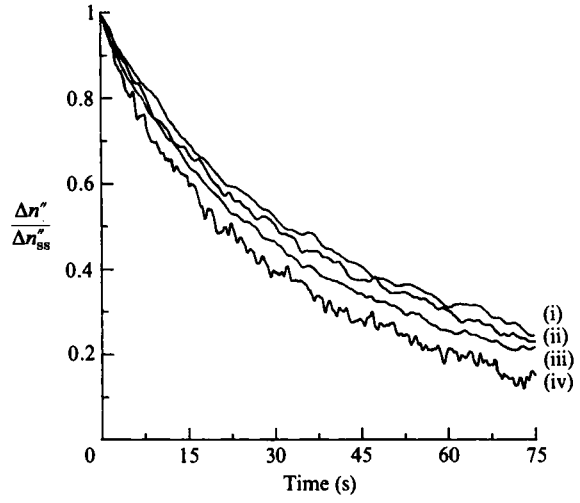

FIGURE 17. Relaxation of the βFeOOH dichroism following sudden cessation of steady simple shear at Pe: (i) 23, (ii) 47, (iii) 94, (iv) 187; normalized by the steady-state dichroism obtained during flow.

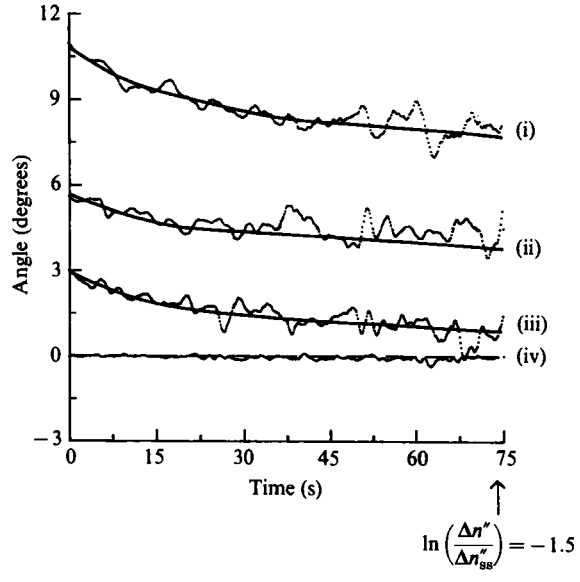

FIGURE 18. Relaxation of the βFeOOH orientation angle (size polydispersity 18 %) following sudden cessation of steady simple shear flow at Pe: (i) 23, (ii) 94, (iii) 187, (iv) 2350. The range of the abscissa corresponds to the time required for $\Delta n''$ to obtain approximately 20 % of its initial value.

βFeOOH and of the bentonite suspensions from steady simple shear. In both figures, the range of the time axis corresponds to the time required for the magnitude of the dichroism signal to decay to approximately 20 % of its initial value. An analogous effect has precedence in the polymer literature where, for example, semi-dilute solutions of stiff, polydispersed collagen protein exhibit decay in the orientation angle (facilitated by the exceptionally strong lengthscale dependence of the diffusivity in

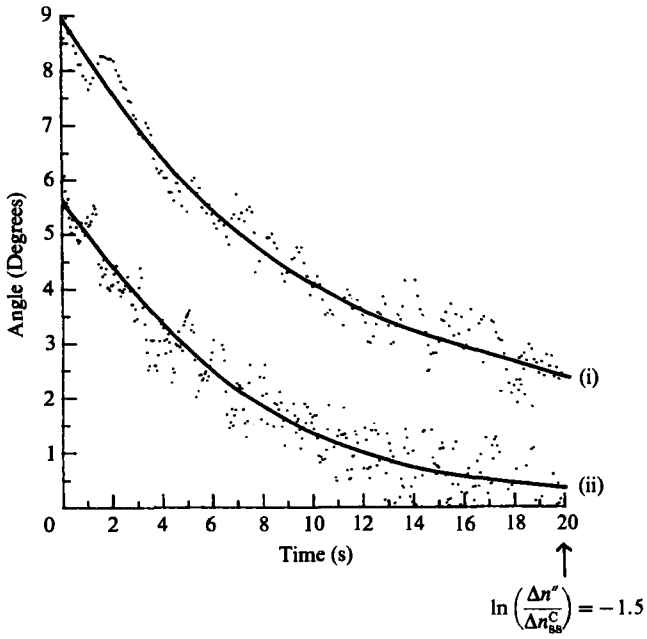

FIGURE 19. Relaxation of the bentonite orientation angle (size polydispersity 57 %) following sudden cessation of steady simple shear flow at Pe: (i) 36, (ii) 72. The range of the abscissa corresponds to the time required for $\Delta n''$ to obtain approximately 20 % of its initial value.

the semi-dilute regime) during relaxation following cessation of steady simple shear (Chow *et al.* 1985).

In figure 18, note first that in the absence of Brownian motion ($Pe > 2300$) the average orientation angle remains constant during relaxation at zero degrees, the value obtained during the flow as a result of the phase-mixing effect induced by aspect-ratio dispersion. At lower Pe, the steady-state angle obtained during flow is non-zero. Following cessation of the flow, the βFeOOH angle decays but only slightly compared to the relaxation of the bentonite data (figure 19) over an equivalent time interval. The enhanced relaxation of the bentonite angle is a consequence of the significantly greater degree of size polydispersity (over three times higher) in the bentonite system than in the synthetic βFeOOH suspension. The possibility of relaxation in the average orientation direction in real particle systems had not been recognized in the past literature. From the results of this and other studies of the flow-inception problem, however, the source of the angle decay phenomena is easily discerned. The magnitude of the steady-state angle obtained during flow increases with decreasing Pe. In a polydispersed suspension sheared at a given $\dot{\gamma}$, the effective Péclet number of the smaller particles of course is lower than the average, and hence these particles obtain a steady angle which exceeds that of the average particle. The converse holds for those particles in the high end of the size distribution. Following cessation of flow, the smaller particles relax more quickly than the average particle. The decay in the average orientation angle then arises simply as a consequence of the fact that as time progresses the smaller particles no longer contribute to the dichroism signal. The averaging process therefore occurs over an effective distribution of particles which has been skewed toward the low-angle side of the distribution initially obtained at the point of flow cessation.

This study was supported in part by grant NSF-CPE8412647 from the National Science Foundation and by a grant from the Petroleum Research Fund of the American Chemical Society. P. L. F. gratefully acknowledges the fellowship support made available to him during the course of this work by the Fannie and John Hertz Foundation.

REFERENCES

ANCZUROWSKI, E. & MASON, S. G. 1967*a* *J. Colloid Interface Sci.* **23**, 522.

ANCZUROWSKI, E. & MASON, S. G. 1967*b* *J. Colloid Interface Sci.* **23**, 533.

ANCZUROWSKI, E., COX, R. G. & MASON, S. G. 1967 *J. Colloid Interface Sci.* **23**, 547.

BIRD, R. B., WARNER, H. R. & EVANS, D. C. 1971 *Adv. Polymer Sci.* **8**, 2–90.

BRENNER, H. 1974 *Intl J. Multiphase Flow* **1**, 195–341.

BRETHERTON, F. P. 1962 *J. Fluid Mech.* **14**, 284–304.

BRUNN, P. 1980 *J. NonNewtonian Fluid Mech.* **7**, 271–288.

CERDA, C. M., FOISTER, R. T. & MASON S. G. 1981 *J. Chem. Soc. Faraday Trans. I*, **77**, 2949–2964.

CHOW, A. W., FULLER, G. G., WALLACE, D. G. & MADRI, J. A. 1985 *Macromolecules* **18**, 793–804.

FRATTINI, P. L. 1985 Thesis. Stanford University.

FRATTINI, P. L. & FULLER, G. G. 1984 *J. Colloid Interface Sci.* **100**(2) 506–518.

JEFFERY, G. B. 1922 *Proc. R. Soc. Lond.* A **102**, 161–179.

HINCH, E. J. & LEAL, L. G. 1972 *J. Fluid Mech.* **52**, 683–712.

HINCH, E. J. & LEAL, L. G. 1973 *J. Fluid Mech.* **57**, 753–767.

HINCH, E. J. & LEAL, L. G. 1975 *J. Fluid Mech.* **71**, 481–495.

HINCH, E. J. & LEAL, L. G. 1976 *J. Fluid Mech.* **76**, 187–208.

KIM, S. 1985 *University of Wisconsin-Madison Mathematics Research Center Technical Summary Report no.* 2790.

KRUSHKAL, E. M. & GALLILY, I. 1984 *J. Colloid Interface Sci.* **99**(1), 141–152.

LEAL, L. G. 1979 *J. NonNewtonian Fluid Mech.* **5**, 33–78.

LEAL, L. G. 1984 *Advances in Rheology, Proceedings of the IXth International Congress on Theology, Mexico*, vol. 1, pp. 191–209.

LEAL, L. G. & HINCH, E. J. 1971 *J. Fluid Mech.* **46**, 685–703.

LEAL, L. G. & HINCH, E. J. 1972 *J. Fluid Mech.* **55**, 745–765.

MATIJEVIC, E. & SCHEINER, P. 1978 *J. Colloid Interface Sci.* **63**, 509–524.

OKAGAWA, A., COX, R. G. & MASON, S. G. 1973 *J. Colloid Interface Sci.* **45**(2) 303–329.

PETERLIN, A. 1976 *Ann. Rev. Fluid Mech.* **8**, 35–55.

SCHERAGA, H. A. 1955 *J. Chem. Phys.* **23**(8) 1526–1532.

SCHERAGA, H. A., EDSALL, J. T. & GADD, J. O., 1951 *J. Chem. Phys.* **19**(9), 1101–1108.

STEWART, W. E. & SØRENSEN, J. P. 1972 *Trans. Soc. Rheol.* **16**(1) 1–13.

VAN DE VEN, T. G. M. 1984 *J. Chem. Soc., Faraday Trans. I*, **80**, 2677–2692.